ChemPhysChem

Research Article
doi.org/10.1002/cphc.202400522

Chemistry Europe
European Chemical Societies Publishing

www.chemphyschem.org

Polymer-Based Room-Temperature Phosphorescence Materials Exhibiting Emission Lifetimes up to 4.6 s Under Ambient Conditions

Xiaoqing Song,[a, b] Xiangxiang Zhai,[a, b] Ying Zeng,[a, b] Guangming Wang,[b] Tengyue Wang,[b] Yufang Li,[c, d] Qianqian Yan,*[b] Chin-Yiu Chan,*[c, d] Biaobing Wang,*[a] and Kaka Zhang*[b]

The long-emission-lifetime nature of room-temperature phosphorescence (RTP) materials lays the foundation of their applications in diverse areas. Despite the advantage of mechanical property, processability and solvent dispersity, the emission lifetimes of polymer-based room-temperature phosphorescence materials remain not particularly long because of the labile nature of organic triplet excited states under ambient conditions. Specifically, ambient phosphorescence lifetime (τ_P) longer than 2 s and even 4 s have rarely been reported in polymer systems. Here, luminescent compounds with small phosphorescence rate on the order of approximately 10^{-1} s^{-1} are designed, ethylene-vinyl alcohol copolymer (EVOH) as polymer matrix and antioxidant 1010 to protect organic triplets are employed, and ultralong phosphorescence lifetime up to 4.6 s under ambient conditions by short-term and low-power excitation are achieved. The resultant materials exhibit high afterglow brightness, long afterglow duration, excellent processability into large area thin films, high transparency and thermal stability, which display promising anticounterfeiting and data encryption functions.

1. Introduction

The long-lived excited state nature is the most important character for organic room-temperature phosphorescence and afterglow materials, compared to fluorescence and metal-complex-based phosphorescence materials.[1] When the emission lifetimes are longer than 0.1 s, mobile phone camera can record afterglow behavior of the materials and even human eyes can distinguish afterglow brightness, afterglow color and their changes. Based on these materials, one can anticipate the emergence of a new platform for optical sensing and analysis, if such materials can effectively conjugate to chemodosimeter technique and supramolecular recognition.

Despite the bright future of room-temperature phosphorescence and organic afterglow materials, the fabrication of such materials with high efficiency and long lifetime remains challenging because of the spin-forbidden nature of triplet population and phosphorescence decay, as well as the weak spin-orbital coupling in organic systems.[2] Pioneering studies in this area showed that heavy atom effect (by the involvement of bromo, iodine and other substituents) and n-π* transition (by the introduction of ketone and aldehyde groups) can facilitate intersystem crossing (ISC) and enhance the population of triplet excited states.[3] These design can also increase the rate of phosphorescence decay (k_P), which is conducive for triplet harvesting and consequently boost phosphorescence efficiency. A possible side effect is the decease of τ_P, according to the equation $\tau_P = 1/(k_P + k_{nr} + k_q)$, where k_{nr} and k_q refer to non-radiative decay constant and oxygen quenching rate constants, respectively. Recent studies show the excellent balance of phosphorescence efficiency and lifetimes in organic systems, whereas long phosphorescence lifetimes, for example, longer than 2 s and even 4 s, remain rarely reported (Figure S1).

The past decade has witnessed tremendous development of two-component design strategy in fabricating room-temperature phosphorescence materials; a second component is employed to control or perturb the photophysical property of luminescent component (the first component).[4] Such strategy requires less synthetic work and allows a flexible combination of both luminophores and second component. Since 2013, our group and other research groups have started the studies of two-component strategy for devising high-performance room-temperature phosphorescence systems.[1g,4a,5] For example, crystalline organic matrices not only suppress intramolecular

[a] X. Song, X. Zhai, Y. Zeng, B. Wang
Jiangsu Key Laboratory of Environmentally Friendly Polymeric Materials
School of Materials Science and Engineering, Jiangsu Collaborative Innovation Center of Photovoltaic Science and Engineering, Changzhou University, Changzhou, China
E-mail: biaobing@cczu.edu.cn

[b] X. Song, X. Zhai, Y. Zeng, G. Wang, T. Wang, Q. Yan, K. Zhang
State Key Laboratory of Organometallic Chemistry and Shanghai Hongkong Joint Laboratory in Chemical Synthesis, Key Laboratory of Synthetic and Self-Assembly Chemistry for Organic Functional Molecules, Ningbo Zhongke creation center of new materials, Shanghai Institute of Organic Chemistry, University of Chinese Academy of Sciences, Chinese Academy of Sciences, 345 Lingling Road, Shanghai 200032, P. R. China
E-mail: yanqianqian@sioc.ac.cn
zhangkaka@sioc.ac.cn

[c] Y. Li, C.-Y. Chan
Department of Materials Science and Engineering, City University of Hong Kong, Tat Chee Avenue, Kowloon, Hong Kong SAR, China

[d] Y. Li, C.-Y. Chan
Department of Chemistry, City University of Hong Kong, Tat Chee Avenue, Kowloon, Hong Kong SAR, China
E-mail: chinychan2@cityu.edu.hk

Supporting information for this article is available on the WWW under https://doi.org/10.1002/cphc.202400522

motion of luminescent component's triplet excited states but also inhibit oxygen diffusion within the matrix to minimize nonradiative decay and oxygen quenching.[6] In other instance where singlet-triplet splitting energy of luminescent component is large than 0.5 eV or even 1.0 eV, suitable organic matrices with T_1 energy levels sandwiched between luminescent component's S_1 and T_1 energy levels have also been reported to mediate ISC of the luminescent component, giving rise to room-temperature phosphorescence materials.[5b,7] Block copolymers have also been used in our studies to modulate the aggregation and photophysical properties of luminescent compounds to form near-infrared crystalline nanostructures with well-defined and uniform morphology.[8] Our recent research has shown that organic matrices such as phenyl benzoate and 4-methoxybenzophenone (with dipole moments in ground state) can perturb luminescent component's S_1 states via dipole-dipole interaction, reduce singlet-triplet splitting energy and thereby enhance ISC.[9] Such dipole effect or medium effect have also been demonstrated by others in well-designed luminescent system and ultrafast time-resolved spectroscopic technique.[10]

Among them, polymer-based room-temperature phosphorescence and afterglow systems have been developed due to their mechanical property, easy processability and good biocompatibility. To the best of our knowledge, room-temperature phosphorescence lifetimes of 2 s have been reported in several polymer-based materials,[11] whereas longer phosphorescence lifetimes (for example, 4 s) have rarely been achieved under ambient conditions (Figure S2). For example, polymethyl methacrylate (PMMA) is frequently used as organic matrix to disperse luminescent component and restrict triplet's nonradiative decay by its glass environment (glass transition temperature of 110 °C), because PMMA is non-expensive, highly transparent and soluble in diverse solvents (for instance, dichloromethane, tetrahydrofuran and toluene).[4a,12] Room-temperature phosphorescence materials in thin-film state and of desired shapes can be obtained by spin-coating, dip-coating and solution casting.[13] It is known that oxygen diffusion in PMMA is relatively fast, which would decrease phosphorescence lifetime in polymer-based system. As a result, room-temperature phosphorescence properties under ambient conditions cannot be turned on by low-power and short-term excitation. Only after enough excitation when the oxygen within PMMA matrix is scavenged, room-temperature phosphorescence can be observed. In addition to PMMA, polyvinyl alcohol, polylactic acid polystyrene, poly(ethylene-co-vinyl acetate), polyacrylonitrile and other rigid polymer matrices have been reported to protect luminescent component's triplet excited states to fabricate polymer-based organic afterglow materials.[14] However, polymer-based RTP system usually have low tolerance to oxygen compared to crystalline materials.

We reason that, besides sufficient population of triplet excited states by ISC, the key to achieve ultralong phosphorescence lifetime is (1) small k_P of around 10^{-1} s^{-1} and (2) very small k_{nr} and k_q. In this study, we first demonstrate one of the most long-lived polymer-based RTP systems by exploring three-component materials with the addition of antioxidant 1010. We select triphenylene-containing compounds featuring small k_P as luminescent dopant, EVOH as polymer matrix to decrease k_P and k_{nr}. Furthermore, the antioxidant 1010 is added to further reduce k_q. Upon doping, the resultant three-component materials display bright afterglow, long afterglow duration and exhibit τ_P over 4 s under ambient conditions with photoluminescence quantum yield (PLQY) of over 40 %. In addition, the fabricated large-area thin films show excellent flexiblity and processability, high transparency and thermal stability, displaying promising anticounterfeiting and data encryption functions.

2. Results and Discussion

2.1. Material Design

Commercially available triphenylen-2-ylboronic acid (TPBA) and triphenylen-2-ylboronic acid pinacol ester (TPBE) are selected as luminescent dopants (Scheme 1). It is known that triphenylene (TP) has small k_P because the spin-forbidden and symmetry-forbidden nature of its T_1-to-S_1 radiative decay, whereas triphenylene shows relatively high-energy absorption band at 260 nm in dichloromethane solution (Figure S3).[15] Excitation source of high energy would be harmful for organic and biological systems. To shift the absorption band to lower-energy region, an easy method is to link electron-withdrawing functional group to triphenylene group, thereby introducing some proportion of intramolecular charge transfer (ICT) character for the S_0-to-S_1 transition, leading to the narrowing of S_0-to-S_1 gap. For instance, TPBA has been found to display absorption bands ranging from 230 to 350 nm in dichloromethane solution (Figure S3). Time-dependent density functional theory (TD-DFT) calculation shows that TPBA's S_1 state has 6.15 % ICT character (because of the presence of electron-withdrawing boronic acid group) plus 93.85 % localized excitation (LE) character (Figure S5, Table S1). Similar UV-vis absorption band and TD-DFT calculation results have been observed in the case of TPBE (Figure S3 and S6). TD-DFT calculations on T_1-to-S_0 transition have also been performed. From the electron-hole isosurface map of T_1 states of both TPBA and TPBE, one can clearly find that their T_1 states are mainly of ^{3}LE characters (97.99 % and 97.88 %, respectively) (Figure S5 and S6, Table S1). Here the triphenylene-containing systems inherit the symmetry-forbidden and spin-forbidden property of pristine triphenylene system. Calculation of phosphorescence rate constants based on Fermi's golden rule rate theory shows that TPBA and TPBE systems have k_P values approximately on the order of 10^{-2} s^{-1} (Table S2). The k_P values obtained by theoretical calculation are smaller than experimental estimation (k_P of around 10^{-1} s^{-1}, *vide infra*), which would be caused by some approximation used in the theoretical methods. Such small k_P values are one of the key points to achieve ultralong phosphorescence lifetimes. Compared with TPBE, TPBA is relatively more expensive. While, TPBE is tend to hydrolysis and TPBA is more stable. Besides, the boronic acid group on TPBA may enhance their interaction with organic matrices through hydrogen bonding or boric acid ester covalent bonds.[15]

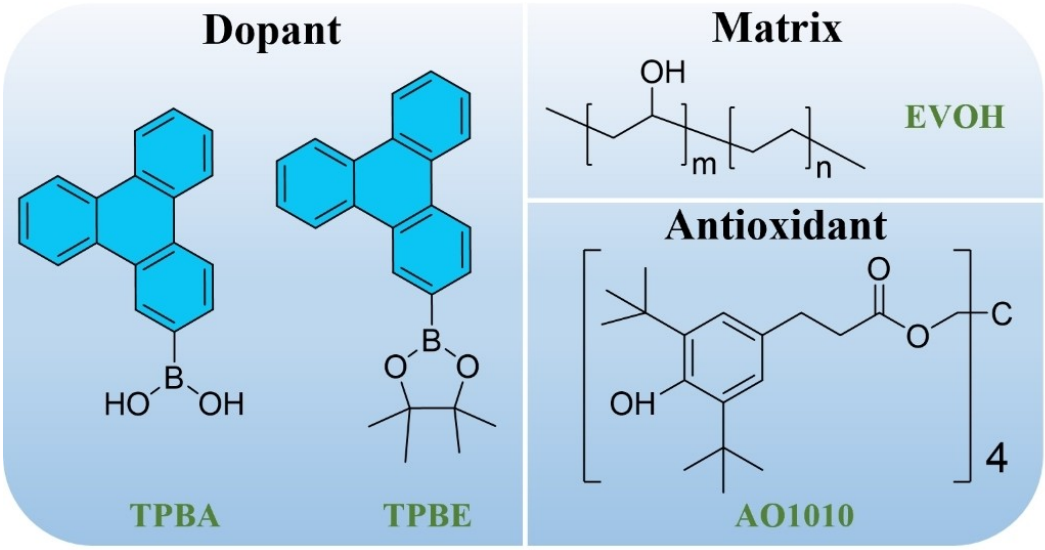

Scheme 1. Chemical structures of the components of the system.

Here EVOH is selected as polymer matrix (Scheme 1). EVOH is transparent and has negligible absorption in UVA and UVB regions. EVOH is moldable (melting point, 150~200 °C) and can also be processed by solution casting technique. Like the reported polymer matrices, EVOH has the capability to suppress intramolecular motion of organic triplet excited states by its rigid microenvironment.[11c,16] It should be noted that the rigid microenvironment for organic triplets doesn't mean that EVOH lack flexibility in its material state; in thin film state, EVOH is very flexible. A distinct feature of EVOH different from common polymers such as PMMA and polystyrene is its strong barrier property against oxygen and gas; because of this, EVOH has been widely used in food packaging. EVOH would inhibit oxygen diffusion within the polymer matrices and efficiently suppress oxygen quenching of organic triplets, which is very important to achieve ultralong-lived phosphorescence lifetimes under ambient conditions. Besides, the rich hydroxyl groups on EVOH can interact luminescent dopants via hydrogen bonding, thereby increasing the miscibility between EVOH and luminescent dopants and further restricting intramolecular motion of organic triplets (that is, decreasing k_{nr} of luminescent dopants' T_1 states).

Besides the molecular design of luminescent dopants and the selection of polymer matrices, we also use antioxidant 1010 (AO1010) as additive to capture oxygen within the matrices and reduce oxygen contents within the matrices (Scheme 1). To our knowledge, such material design by adding sacrificing agents have rarely been reported in previous studies. The presence of antioxidant 1010 can further suppress oxygen quenching of luminescent dopants' T_1 states, which would be beneficial for fabricating materials with long phosphorescence lifetimes.

2.2. Material Preparation and Photophysical Properties

The three-component RTP materials were prepared based on dip-casting method. The mixed solution of EVOH, TPBA (or TPBE, 1 wt%) and AO1010 (0.3 wt%) was coated on a polyethylene terephthalate (PET) substrate, followed by the evaporation of the solvent. The TPBA-EVOH-AO1010 and TPBE-EVOH-AO1010 films show intense blue emission under 365 nm UV light excitation and exhibit blue afterglow with the duration of 42 s and 30 s, respectively (Figure 1A–B).

The photophysical properties of the films were studied under ambient conditions. The steady-state emission spectra of the TPBA-EVOH-AO1010 and TPBE-EVOH-AO1010 exhibit similar emission bands ranging from 350 to 600 nm with a maximum wavelength at 373 nm (Figure 1C). Their delayed emission spectra (1 ms delay) display phosphorescence maxima at 476 nm, as well as shoulders at 448 and 507 nm, which can be assigned to the vibronic transition from T_1 excited state to different vibrational energy levels of ground state (Figure 1C), consistent with their blue emission afterglow. When the excitation wavelength varies from 220 to 360 nm, the emission bands show no shift (Figure S7), suggesting that the phosphorescence emission is stable under UV light excitation. The phosphorescence lifetime monitored at 458 nm of TPBE-EVOH-AO1010 is 4.46 s (Figure 1D). While, the TPBA-EVOH-AO1010 film has longer τ_P up to 4.61 s (Figure 1D). It has been reported that the dynamic formation of boronic ester between boronic acid and polyhydroxy polymer can occurs in alkaline solution.[17] It' s not the case in the present study. Compared with TPBE, the TPBA with -B(OH_2) groups, which contain both electron doner O and electron acceptor H, tends to form relatively strong hydron bonds with -OH groups.[15,18] Therefore, we proposed that it contributed to the hydrogen bonding between boronic acid group on TPBA and hydroxyl groups on EVOH, which further restricts the motion of the molecules. The PLQYs of the TPBA-

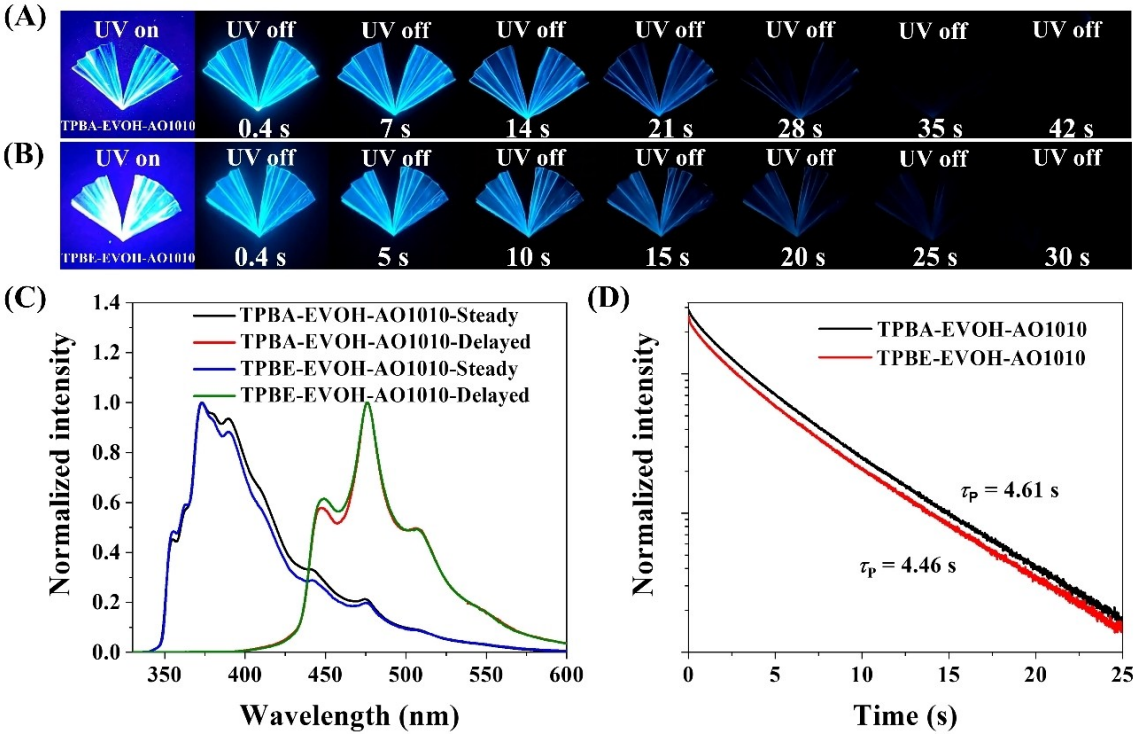

Figure 1. Photographs of (A) TPBA-EVOH-AO1010 and (B) TPBE-EVOH-AO1010 films under 365 nm UV excitation (5 W) and after ceasing the light source. (C) Room-temperature steady-state, delayed emission (1 ms delay) spectra and (D) decay profiles (monitored at 458 nm) of TPBA-EVOH-AO1010 and TPBE-EVOH-AO1010 films.

EVOH-AO1010 and TPBE-EVOH-AO1010 under ambient conditions were measured to be 41% and 36%, respectively. The photophysical properties of the materials are summarized in Table S3.

The fluorescence/phosphorescence dual emission is observed from the steady-state emission spectra of the films at 77 K (Figure S8), implying that the luminophores have strong ISC tendency. The delayed emission spectra of the materials measured at 77 K exhibit similar emission bands and maxima to the spectra at room temperature (Figure 2A–B), confirming that the 400–600 nm emission bands originate from phosphorescence. In the reported studies, the emergence of organic room-temperature phosphorescence and afterglow can be produced by impurity mechanism,[19] matrices' T_1 mediation mechanism,[7,20] triplet-to-triplet energy transfer (TTET),[21] organic long persistant luminescence (OLPL).[5g,22] (1) The purity of the dopants is demonstrated by HPLC (Figure S10), thus, the impurity mechanism can be ruled out. (2) It is reported that the organic matrices' T_1 states with energy levels sandwiched between S_1 and T_1 states of dopants would mediate the singlet-to-triplet ISC of the luminescent dopants, giving rise to strong room-temperature organic afterglow.[7,20] Since the T_1 level of EVOH is much higher than TPBA's S_1 and T_1 states, the matrices' T_1 mediation mechanism is not the case in the present study. (3) When the matrices can be sufficiently excited, the triplet-to-triplet energy transfer (TTET) from organic matrices to dopants may lead to the emergence of RTP.[1h,4d,23] While EVOH possess negligible UV-vis absorption at 365 nm and the TPBA-EVOH-AO1010 shows bright afterglow after 365 nm irradiation, TTET mechanism can be ruled out. (4) Intermolecular charge transfer between dopants and matrices is not favored due to EVOH matrices possess much higher-lying LUMO and lower-lying HOMO compared to TPBA dopants.[13b,15]

Compared with the dopant-matrix RTP materials based on other polymers (such as PMMA), which need long-term irradiation to eliminate oxygen and realize room-temperature phosphorescence, the afterglow of dopant-EVOH materials can be easily observed after a few seconds of low-power irradiation due to the excellent oxygen-barrier property of EVOH, decreasing the oxygen diffusion rate. In addition, the AO1010 was added to decrease the concentration of oxygen, further suppressed the k_q. Meanwhile, there is a very low probability of collision between small amount of AO1010 and luminescent molecules, avoilding queching of the triplet states of luminophores. In order to demonstrate the vital role of the AO1010, two-component TPBA-EVOH and TPBE-EVOH materials were also prepared through the same procedures. Their room-temperature steady-state emission and delayed emission spectra show similar bands with TPBA-EVOH-AO1010 and TPBE-EVOH-AO1010 (Figure S11D). As expected, their phosphorescence lifetimes are shorter than those of three-component materials (Figure S11E), proving the presence of AO1010 can further suppress the oxygen quenching of luminescent dopants' T_1 states and leads to a smaller k_q. The k_P value of the TPBA-EVOH-AO1010 and TPBE-EVOH-AO1010 are evaluated to be approximately 0.9×10^{-1} s^{-1} from the decay spectra of the films

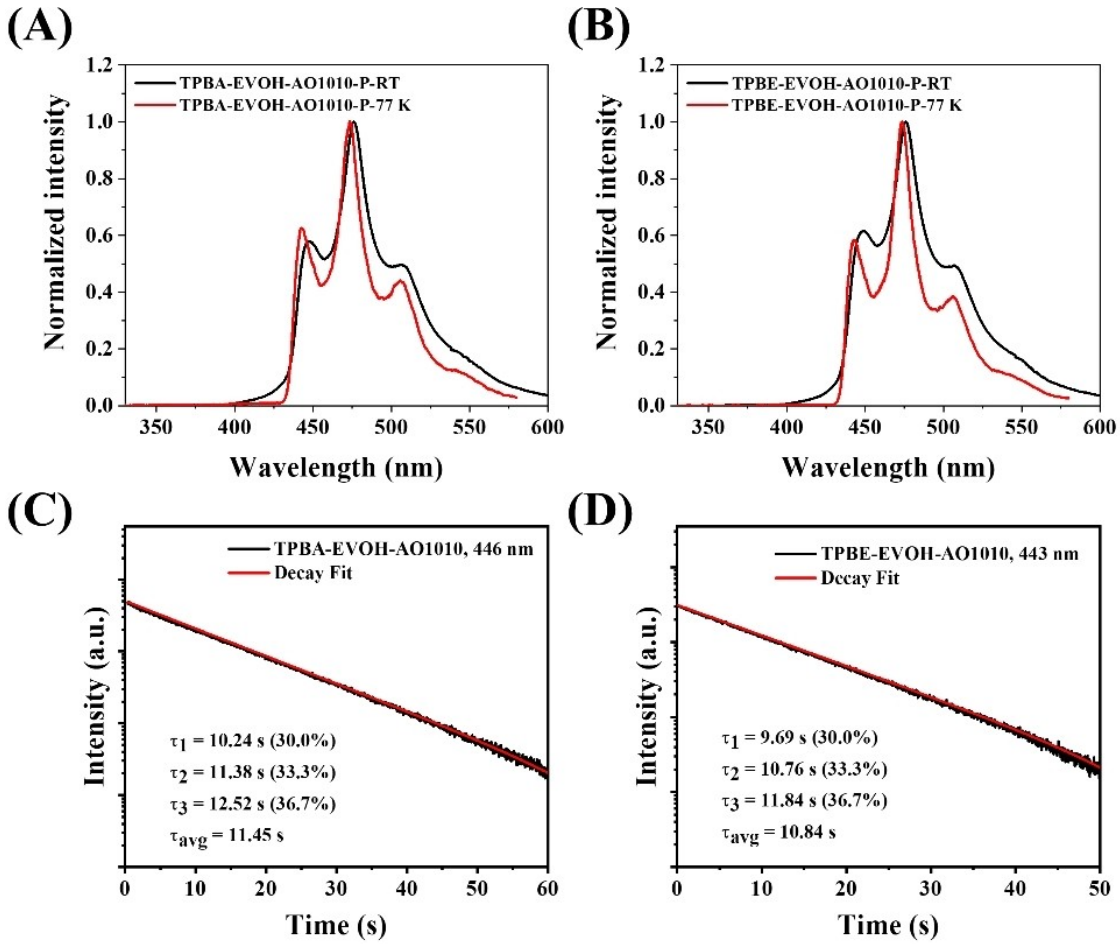

Figure 2. The delayed emission (1 ms delay) spectra of (A) TPBA-EVOH-AO1010 and (B) TPBE-EVOH-AO1010 at room temperature and 77 K. Decay profiles of (C) TPBA-EVOH-AO1010 (monitored at 446 nm) and (D) TPBE-EVOH-AO1010 films (monitored at 443 nm).

at 77 K, contributed to TP moieties. It is consistent with their k_P value obtained by TD-DFT calculations in order of magnitude. The $k_{nr}+k_q$ of the dopants can be suppressed by EVOH, and AO1010 further suppressed the k_q. Based on the cooperative effects of multi-component, the $k_P+k_{nr}+k_q$ value at room temperature is evaluated merely $2\times10^{-1}\ s^{-1}$. As a result, ultra-long τ_P up to 4.6 s, which has rarely been reported, is realized.

Besides, the Powder X-ray diffraction (PXRD) patterns of the films indicate their crystalline nature (Figure 3A). Furthermore, differential scanning calorimetry (DSC) measurements were carried out. The melting points (T_m) of TPBA-EVOH-AO1010 and TPBE-EVOH-AO1010 were measured to be 170.3 °C (Figure 3B). And their glass transition temperature (T_g) was measured to be 55.2 and 49.8 °C, respectively (Figure 3C). The TPBA-EVOH-AO1010 with higher T_g than TPBE-EVOH-AO1010 and EVOH is attributed to enhancement of the rigidity of the system by the relatively strong hydrogen bonding between the boronic acid group on TPBA and hydroxyl groups on EVOH.[15,24] Thermogravimetric analysis (TGA) show that those films have high thermal stability (Figure 3D). UV-vis spectra of the films display similar absorption bands to the TPBA/TPBE, further confirmed the existence of the luminescent dopant (Figure S12A). Transmittance of the films remains 80–90% in visible region (Figure S12B). The above results show the high-performance of the afterglow films.

2.3. Material Functions

The obtained large-area thin films TPBA-EVOH-AO1010 and TPBE-EVOH-AO1010 are highly transparent (Figure 4A) and flexible (Figure 4B). Owing to their excellent processability and flexibility, diverse afterglow patterns were fabricated by folding the films (Figure 4C–D). Atomic force microscopy (AFM) results indicate that the surface of the film, which possesses very small average surface roughness (Ra), is very smooth (Figure 4E–F).

In view of long τ_P, excellent processability and flexibility of the large-area afterglow films, we further explored their application in anticounterfeiting and data encryption (Figure 5). As shown in Figure 5A, the character of "1978" was written on a postcard by using the mixed solution of TPBA, EVOH and AO1010. And the solution of EVOH was added to modify "9" to "8". Only "1878" can be seen in daylight and it exhibits intense emission under 365 nm UV light. While "1978" was observed after turning off the UV lamp. Similarly, when other characters were written by the TPBA-EVOH-AO1010 solution and EVOH

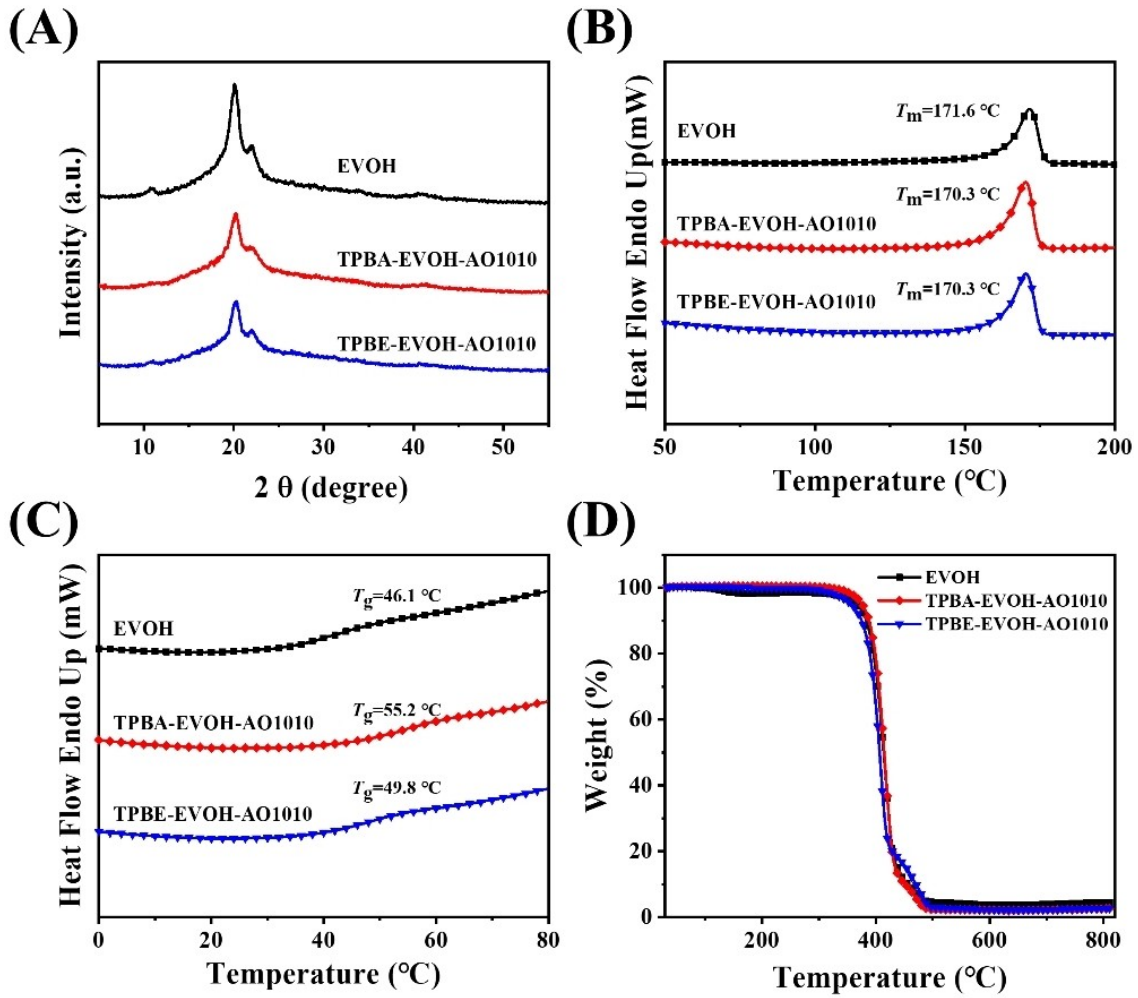

Figure 3. (A) XRD (B, C) DSC and (D) TGA measurements of TPBA, TPBA-EVOH-AO1010 and TPBE-EVOH-AO1010 films.

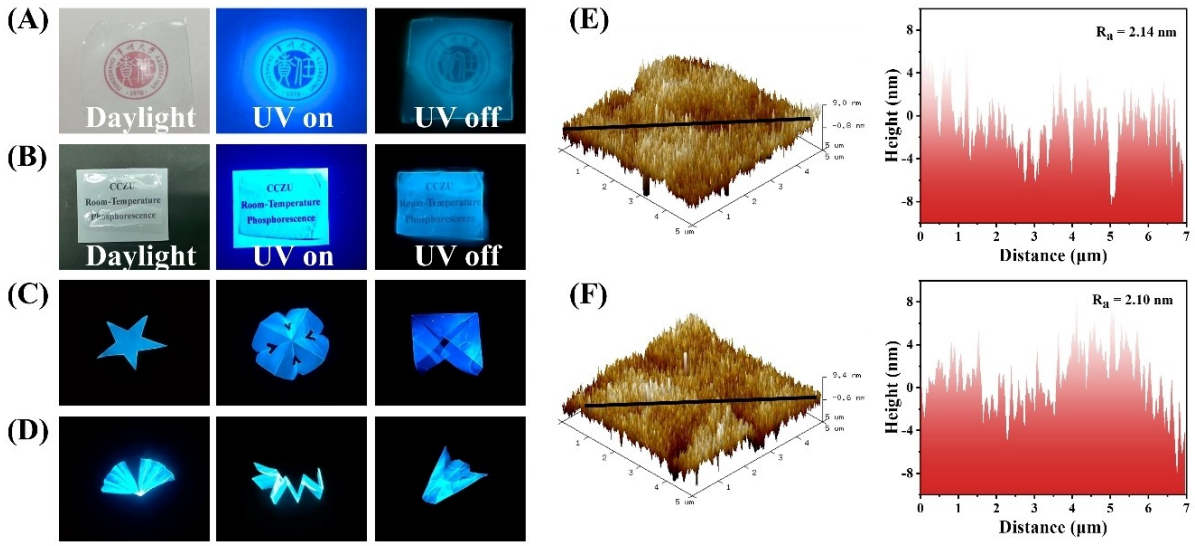

Figure 4. Transparency of (A) TPBA-EVOH-AO1010 and (B) TPBE-EVOH-AO1010 films. (B) Flexibility of (C) TPBA-EVOH-AO1010 and (D) TPBE-EVOH-AO1010 films. 3D AFM images and corresponding cross-sectional analysis along the black lines for (E) TPBA-EVOH-AO1010 and (F) TPBE-EVOH-AO1010 films.

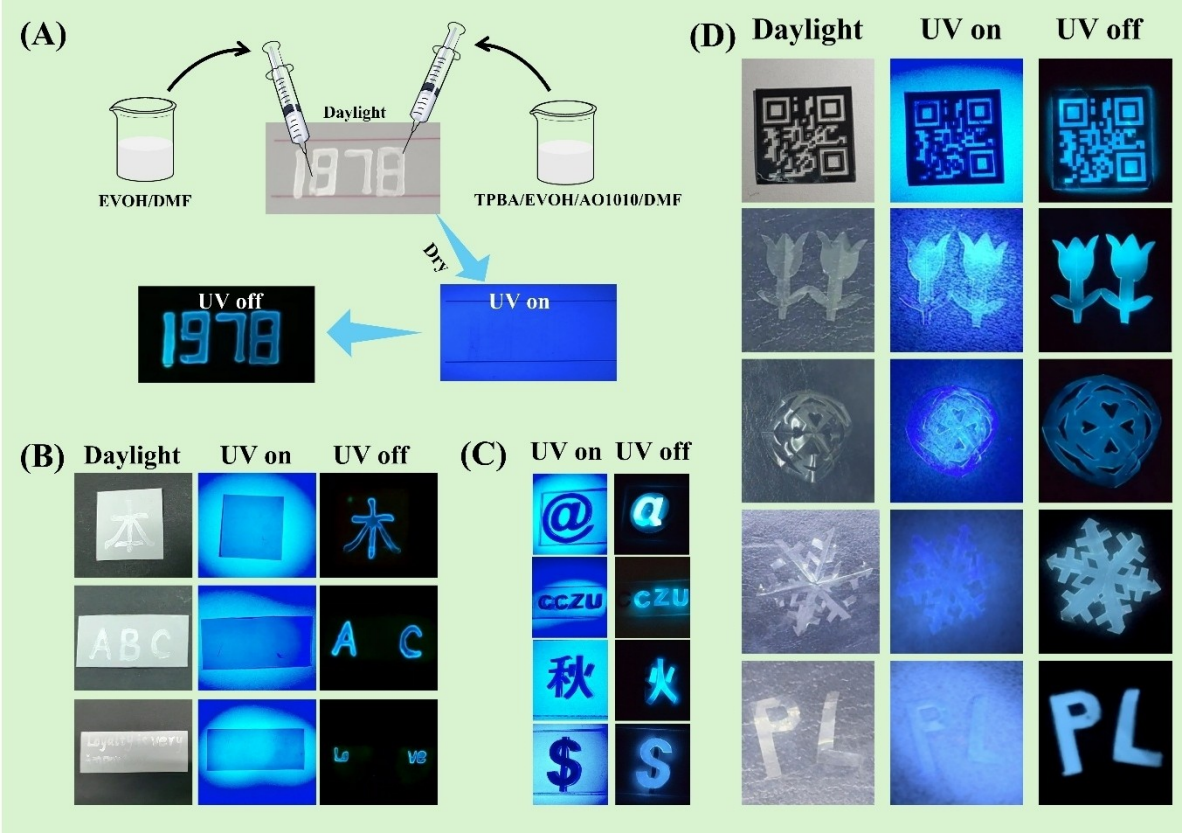

Figure 5. (A–B) Graphical representation and photographs of afterglow materials prepared from the solution of the solution of EVOH and the mixed solution of TPBA, EVOH and AO1010 for anticounterfeiting and data encryption. (C) The TPBA-EVOH-AO1010 films were processed into various afterglow patterns and used for data encryption with the aid of paper-cut model. (D) The TPBA-EVOH-AO1010 film were processed into various afterglow patterns and used for anticounterfeiting and data encryption.

solution, a different character were observed after ceasing the UV light sources (Figure 5B). Besides, the 5×5 cm TPBA-EVOH-AO1010 films were processed into various afterglow patterns and used for data encryption with the aid of paper-cut model (Figure 5C). More transparent patterns were obtained owing to their excellent processability and can be used for the anticounterfeiting (Figure 5D). The QR code on the TPBA-EVOH-AO1010 film can be successfully scanned when the UV light is off (Figure 5D). The above results demonstrated the potential applications of these afterglow materials in anticounterfeiting and data encryption.

3. Conclusions

In conclusion, we report a kind of polymer-based afterglow materials exhibiting high afterglow brightness and ultralong lifetimes up to 4.6 s under ambient conditions. The luminescent TPBA and TPBE compounds possess small k_P. The semi-crystalline EVOH matrix with oxygen-barrier characteristic provides a rigid environment. Besides, the antioxidant 1010 is first proved to further protect the excited states of the luminophores. The cooperative effects lead to the high-performance afterglow materials. In addition, the afterglow materials with excellent processability and high transparency can be used to fabricate large-area transparent flexible films, displaying promising anticounterfeiting and data encryption functions.

Acknowledgements

We acknowledge the financial support from the National Natural Science Foundation of China (22175194), the Strategic Priority Research Program of the Chinese Academy of Sciences (XDB0610000), the Hundred Talents Program from the Shanghai Institute of Organic Chemistry (Y121078), the Pioneer Hundred Talents Program of the Chinese Academy of Sciences (E320021), and the Ningbo Natural Science Foundation (2023 J243). C.-Y. Chan thanks the financial support from the City University of Hong Kong (Project No. 9610637 and 9231531).

Conflict of Interests

The authors declare no conflict of interest.

Data Availability Statement

The data that support the findings of this study are available from the corresponding author upon reasonable request.

Keywords: Phosphorescence · Polymer · Afterglow · Triphenylene · Anticounterfeiting

[1] a) V. W. W. Yam, V. K. M. Au, S. Y. L. Leung, *Chem. Rev.* **2015**, *115*, 7589; b) W. Zhao, Z. He, B. Z. Tang, *Nat. Rev. Mater.* **2020**, *5*, 869; c) N. Gan, H. F. Shi, Z. F. An, W. Huang, *Adv. Funct. Mater.* **2018**, *28*, 1802657; d) Q. Q. Li, Z. Li, *Acc. Chem. Res.* **2020**, *53*, 962–973; e) Kenry, C. J. Chen, B. Liu, *Nat. Commun.* **2019**, *10*, 2111; f) X. Ma, J. Wang, H. Tian, *Acc. Chem. Res.* **2019**, *52*, 738–748; g) R. Kabe, C. Adachi, *Nature* **2017**, *550*, 384–387; h) S. Hirata, *Adv. Opt. Mater.* **2017**, *5*, 1700116.

[2] a) T. T. Li, Y. Zheng, C. Q. Wu, C. Y. Yan, C. Zhang, H. Gao, Q. Chen, K. Zhang, *Chin. Chem. Lett.* **2022**, *33*, 4238–4242; b) G. Q. Zhang, G. Palmer, M. Dewhirst, C. Fraser, *Nat. Mater.* **2009**, *8*, 747; c) J. Y. Li, G. M. Wang, X. F. Chen, X. Li, M. J. Wu, S. Yuan, Y. L. Zou, X. P. Wang, K. K. Zhang, *Chem. Eur. J.* **2022**, *28*, e202200852; d) Y. Y. Si, Y. Y. Zhao, W. B. Dai, S. S. Cui, P. Sun, J. B. Shi, B. Tong, Z. X. Cai, Y. P. Dong, *ACS Mater. Lett.* **2021**, *3*, 379; e) T. Zhang, X. Ma, H. W. Wu, L. L. Zhu, Y. L. Zhao, H. Tian, *Angew. Chem. Int. Ed.* **2020**, *59*, 11206; f) M. Singh, K. Liu, S. L. Qu, H. L. Ma, H. F. Shi, Z. F. An, W. Huang, *Adv. Opt. Mater.* **2021**, *9*, 2002197.

[3] a) Z. H. He, H. Q. Gao, S. T. Zhang, S. Y. Zheng, Y. Z. Wang, Z. H. Zhao, D. Ding, B. Yang, Y. M. Zhang, W. Z. Yuan, *Adv. Mater.* **2019**, *31*, 1807222; b) S. Y. Sun, L. W. Ma, J. Wang, X. Ma, H. Tian, *Natl. Sci. Rev.* **2021**, *9*, nwab085; c) J. G. Wang, X. G. Gu, H. L. Ma, Q. Peng, X. B. Huang, X. Y. Zheng, S. H. P. Sung, G. G. Shan, J. W. Y. Lam, Z. Shuai, B. Z. Tang, *Nat. Commun.* **2018**, *9*, 2963; d) J. Yang, X. Zhen, B. Wang, X. M. Gao, Z. C. Ren, J. Q. Wang, Y. J. Xie, J. R. Li, Q. Peng, K. Y. Pu, *Nat. Commun.* **2018**, *9*, 840; e) Y. Tao, R. F. Chen, H. H. Li, J. Yuan, Y. F. Wan, H. Jiang, C. L. Chen, Y. B. Si, C. Zheng, B. C. Yang, *Adv. Mater.* **2018**, *30*, 1803856; f) L. T. Xu, G. P. Li, T. Xu, W. D. Zhang, S. K. Zhang, S. W. Yin, Z. F. An, G. He, *Chem. Commun.* **2018**, *54*, 9226.

[4] a) F. Gu, T. Jiang, X. Ma, *ACS Appl. Mater. Interfaces* **2021**, *13*, 43473–43479; b) J. J. Bai, G. K. Dai, H. W. Jin, J. X. Ma, Z. W. Li, Y. Guan, M. X. Chen, Z. M. Ma, Z. Y. Ma, *J. Mater. Chem. C* **2023**, *11*, 16325; c) Y. F. Zhang, Q. K. Sun, L. T. Yue, Y. G. Wang, S. W. Cui, H. C. Zhang, S. F. Xue, W. J. Yang, *Adv. Sci.* **2022**, *9*, 2103402; d) S. Kuila, S. J. George, *Angew. Chem. Int. Ed.* **2020**, *59*, 9393–9397; e) J. H. Yang, X. H. Wu, J. B. Shi, B. Tong, Y. X. Lei, Z. X. Cai, Y. P. Dong, *Adv. Funct. Mater.* **2021**, *31*, 2108072; f) Z. Lin, R. Kabe, N. Nishimura, K. Jinnai, C. Adachi, *Adv. Mater.* **2018**, *30*, 1803713.

[5] a) Y. Sun, G. Wang, X. Li, B. Zhou, K. Zhang, *Adv. Opt. Mater.* **2021**, *9*, 2100353; b) B. Chen, W. Huang, X. Nie, F. Liao, H. Miao, X. Zhang, G. Zhang, *Angew. Chem. Int. Ed.* **2021**, *60*, 16970–16973; c) P. Alam, N. L. C. Leung, J. Liu, T. S. Cheung, X. Zhang, Z. He, R. T. K. Kwok, J. W. Y. Lam, H. H. Y. Sung, I. D. Williams, C. C. S. Chan, K. S. Wong, Q. Peng, B. Z. Tang, *Adv. Mater.* **2020**, *32*, 2001026; d) X. Li, G. M. Wang, J. Y. Li, Y. Sun, X. J. Deng, K. K. Zhang, *ACS Appl. Mater. Interfaces* **2022**, *14*, 1587–1600; e) S. Xu, W. Wang, H. Li, J. Y. Zhang, R. F. Chen, S. Wang, C. Zheng, G. C. Xing, C. Y. Song, W. Huang, *Nat. Commun.* **2020**, *11*, 4802; f) W. B. Li, Z. N. Li, C. F. Si, M. Y. Wong, K. Jinnal, A. K. Gupta, R. Kabe, C. Adachi, W. Huang, E. Zysman-Colman, I. D. W. Samuel, *Adv. Mater.* **2020**, *32*, 2003911; g) Z. Y. Zhang, Y. Chen, Y. Liu, *Angew. Chem. Int. Ed.* **2019**, *58*, 6028–6032; h) K. Jinnai, R. Kabe, Z. Lin, C. Adachi, *Nat. Mater.* **2022**, *21*, 338–344; i) S. Hirata, K. Totani, J. Zhang, T. Yamashita, H. Kaji, S. R. Marder, T. Watanabe, C. Adachi, *Adv. Funct. Mater.* **2013**, *23*, 3386; j) X. X. Zhai, Y. Zeng, X. J. Deng, Q. Q. Lou, A. Z. Cao, L. M. Ji, Q. Q. Yan, B. B. Wang, K. K. Zhang, *Chem. Commun.* **2023**, *59*, 10500.

[6] a) Y. Y. Wu, L. Liu, J. H. Zou, J. Q. Liu, Y. C. Hu, C. Y. Ban, F. Y. Li, Z. F. Li, H. S. Zhang, Z. Zhou, J. F. Zhao, F. Xiu, X. Huang, Q. Zhao, M. Eginligil, W. Huang, *Adv. Opt. Mater.* **2022**, *10*, 2102323; b) G. He, B. D. Wiltshire, P. Choi, A. Savin, S. Sun, A. Mohammadpour, M. J. Ferguson, R. McDonald, S. Farsinezhad, A. Brown, *Chem. Commun.* **2015**, *51*, 5444.

[7] S. Guo, W. B. Dai, X. A. Chen, Y. X. Lei, J. B. Shi, B. Tong, Z. X. Cai, Y. P. Dong, *ACS Mater. Lett.* **2021**, *3*, 379–397.

[8] K. K. Zhang, M. C. L. Yeung, S. Y. L. Leung, V. W. W. Yam, *Proc. Natl. Acad. Sci. U. S. A.* **2017**, *114*, 11844–11849.

[9] a) M. J. Wu, X. P. Wang, Y. T. Pan, J. Y. Li, X. Li, Y. Sun, Y. L. Zou, H. F. Zhang, K. K. Zhang, *J. Phys. Chem. C.* **2021**, *125*, 26986; b) J. H. Liu, G. M. Wang, X. P. Wang, Y. Sun, B. Zhou, Y. L. Zou, B. B. Wang, K. K. Zhang, *Chem. Eur. J.* **2021**, *27*, 16735–16743; c) X. P. Wang, Y. Sun, G. M. Wang, J. Y. Li, X. Li, K. K. Zhang, *Angew. Chem. Int. Ed.* **2021**, *60*, 17138.

[10] a) Z. S. Yoon, M. C. Yoon, D. Kim, *J. Photoch. Photobio. C.* **2005**, *6*, 249–263; b) Y. Liu, N. Xiao, N. Q. Gong, H. Wang, X. Shi, W. Gu, L. Ye, *Carbon* **2014**, *68*, 258–264.

[11] a) B. Wu, N. N. Guo, X. T. Xu, Y. M. Xing, K. Shi, W. H. Fang, G. J. Wang, *Adv. Opt. Mater.* **2020**, *8*, 2001192; b) D. Li, Y. J. Yang, J. Yang, M. M. Fang, B. Z. Tang, Z. Li, *Nat comm.* **2022**, *13*, 347; c) H. Thomas, D. L. Pastoetter, M. Gmelch, T. Achenbach, A. Schlögl, M. Louis, X. L. Feng, S. Reineke, *Adv. Mater.* **2020**, *32*, 2000880.

[12] D. Lee, O. Bolton, B. C. Kim, J. H. Youk, S. Takayama, J. Kim, *J. Am. Chem. Soc.* **2013**, *135*, 6325–6329.

[13] a) S. Ma, H. Y. Ma, K. Yang, Z. N. Tan, B. Zhao, J. P. Deng, *ACS Nano* **2023**, *17*, 6912–6921; b) D. M. Guo, Y. Y. Wang, J. Z. Chen, Y. F. Cao, Y. L. Miao, H. H. Huang, Z. G. Chi, Z. Y. Yang, *Chin. Chem. Lett.* **2023**, *34*, 107882.

[14] a) H. Thomas, K. Haase, T. Achenbach, T. Bärschneider, A. Kirch, F. Talnack, S. C. B. Mannsfeld, S. Reineke, *Front. Phys.* **2022**, *10*, 841413; b) Y. F. Zhang, Y. Su, H. W. Wu, Z. H. Wang, C. Wang, Y. Zheng, X. Zheng, L. Gao, Q. Zhou, Y. Yang, X. H. Chen, C. L. Yang, Y. L. Zhao, *J. Am. Chem. Soc.* **2021**, *143*, 13675–13685; c) C. DeRosa, J. Samonina-Kosicka, Z. Y. Fan, H. Hendargo, D. Weitzel, G. Palmer, C. Fraser, *Macromolecules* **2015**, *48*, 2967–2977; d) H. Z. Wu, D. L. Wang, Z. Zhao, D. Wang, Y. Xiong, B. Z. Tang, *Adv. Funct. Mater.* **2021**, *31*, 2101656.

[15] F. X. Lin, H. Y. Wang, Y. F. Cao, R. J. Yu, G. D. Liang, H. H. Huang, Y. X. Mu, Z. Y. Yang, Z. G. Chi, *Adv. Mater.* **2022**, *34*, 2108333.

[16] Y. Zhu, M. Y. He, L. J. Qu, Y. K. Wang, C. Li, J. Y. Huang, Q. G. Chen, C. L. Yang, *Small* **2023**, *20*, e2309081.

[17] a) R. Tian, S. M. Xu, Q. Xu, C. Lu, *Sci. Adv.* **2020**, *6*, eaaz6107; b) X. K. Ma, Q. W. Cheng, X. L. Zhou, Y. Liu, *JACS Au* **2023**, *3*, 2036.

[18] Y. Su, Y. F. Zhang, Z. H. Wang, W. C. Gao, P. Jia, D. Zhang, C. L. Yang, Y. B. Li, Y. L. Zhao, *Angew. Chem. Int. Ed.* **2020**, *59*, 9967.

[19] a) H. Xiao, D. S. Zheng, L. Y. Zhang, L. J. Xu, Z. N. Chen, *Adv. Funct. Mater.* **2023**, *33*, 2214241; b) W. G. Qiao, M. Yao, J. W. Xu, H. Y. Peng, J. L. Xia, X. L. Xie, Z. N. Li, *Angew. Chem. Int. Ed.* **2023**, *62*, e2023159; c) C. J. Chen, Z. G. Chi, K. C. Chong, A. S. Batsanov, Z. Yang, Z. Mao, Z. Y. Yang, B. Liu, *Nat. Mater.* **2021**, *20*, 175; d) Q. Sun, J. J. Ren, Q. Peng, Z. G. Shuai, *Adv. Opt. Mater.* **2023**, *12*, 2301769.

[20] Y. X. Lei, W. B. Dai, J. X. Guan, S. Guo, F. Ren, Y. D. Zhou, J. B. Shi, B. Tong, Z. X. Cai, J. R. Zhang, Y. P. Dong, *Angew. Chem. Int. Ed.* **2020**, *59*, 16054.

[21] a) S. Y. Kim, J. W. Yu, S. Choi, D. W. Cho, C. H. Kim, H. J. Son, S. O. Kang, *Inorg. Chem.* **2023**, *62*, 14228–14242; b) C. H. Shi, J. Yao, X. R. Wang, X. Wen, W. Y. Shi, C. Lu, *J. Mater. Chem. C.* **2019**, *7*, 14170–14180; c) M. E. Olumba, R. M. O'Donnell, T. N. N. J. R. Rohrabaugh, T. S. Teets, *Inorg. Chem.* **2023**, *62*, 13702–13711.

[22] a) X. Liang, X. F. Luo, Z. P. Yan, Y. X. Zheng, J. L. Zuo, *Angew. Chem. Int. Ed.* **2021**, *60*, 24437–24442; b) X. Liang, Y. X. Zheng, J. L. Zuo, *Angew. Chem. Int. Ed.* **2021**, *60*, 16984–16988; c) Z. S. Lin, R. Kabe, N. Nishimura, K. Jinnai, *C, Adv. Mater.* **2018**, *30*, 1803713.

[23] a) J. X. Wang, H. Zhang, L. Y. Niu, X. Zhu, Y. F. Kang, R. Boulatov, Q. Z. Yang, *CCS Chem.* **2020**, *2*, 1391–1398; b) Q. Dang, Y. Jiang, J. Wang, J. Wang, Q. Zhang, M. Zhang, S. Luo, Y. Xie, K. Pu, Q. Li, Z. Li, *Adv. Mater.* **2020**, *32*, 2006752; c) K. Jinnai, R. Kabe, C. Adachi, *Adv. Mater.* **2018**, *30*, 1800365.

[24] R. G. M. van der Sman, *J. Phys. Chem. B* **2013**, *117*, 16303..

Manuscript received: May 16, 2024
Revised manuscript received: June 13, 2024
Accepted manuscript online: August 14, 2024
Version of record online: October 22, 2024